Pergamon

PII: S0191–8141(98)00004–2

Journal of Structural Geology, Vol. 20, No. 6, pp. 661 to 672, 1998

0191-8141/98 $19.00 + 0.00

Physical experiments of transpressional folding

BASIL TIKOFF* and KARL PETERSON

Department of Geology and Geophysics, University of Minnesota, Minneapolis, MN 55455, U.S.A.

(*Received* 28 *March* 1997; *accepted in revised form* 7 *January* 1998)

Abstract—In order to understand the process of folding in obliquely convergent settings, we formed folds within a shear box capable of creating homogeneous transpressional deformations. Folds were created in a single layer of stiff mixed plasticine and silicone that overlay a Newtonian silicone, for a variety of plate convergence angles. As small amplitude folds became visible, they were parallel to the long axis of the horizontal finite strain ellipse. With increasing deformation, the fold hinges rotated parallel with the long axis of the horizontal finite strain ellipse for all angles of convergence. This parallelism indicates that fold hinges, once formed, rotate with the horizontal strain ellipse rather than as material lines.

The experiments highlight several interesting effects of transpression dynamics. The fold hinges initiate parallel to either $\dot{s}_1$ or $\dot{s}_2$ and are parallel to either S_1 or S_2 with increasing deformation. Neither infinitesimal strain (stress) nor finite strain is resolvable solely from fold geometry. Further, the net amount of contraction determined by folding across the zone was overestimated in all cases except pure contraction. This effect is obvious for the case of wrenching, where folding implies that the zone contracts if elongation parallel to the fold hinge is not considered. Therefore, attempts to balance cross-sections in transpressional zones will tend to overestimate contraction unless the wrench component of deformation is addressed. This result is validated by applying the modeling results in folding in central California adjacent to the San Andreas fault, where cross-section balancing indicates higher amounts of contraction than predicted by plate motion. © 1998 Elsevier Science Ltd. All rights reserved

INTRODUCTION

Harland (1971) used the term "transpression" to define obliquely convergent plate interaction and further recognized that folding is relatively common in this tectonic setting. The character of the folds is such that they may initiate at relatively high angles to the plate boundary, but rotate into parallelism with increasing deformation. The existence of en échelon folds in wrench zones, often adjacent to strike-slip faults, brought further attention to the development of folds with a large simple shear component of deformation (e.g. Wilcox *et al.*, 1973). The common observation was that these folds were oriented at less than 45° to the adjacent strike-slip fault. However, it was not clear whether the folds initiated at 45° and subsequently rotated, or whether they initiated at a lower angle. The latter, as suggested by Sanderson and Marchini (1984), would indicate a combination of contraction and wrenching across the zone. Their model of transpression—oblique convergence with no lateral extrusion—began the process of quantifying the process of three-dimensional folding in such tectonic settings.

However, there remained two primary questions about folding in transpression: (1) At what angle do the folds initiate?; and (2) Once formed, do fold hinges rotate as material lines or with the finite strain ellipse? Kinematic work suggested that the folds should initiate perpendicular to the infinitesimal shortening axis (or shortest infinitesimal strain axis) in the plane of the layer (Flinn, 1962; Treagus and Treagus, 1992). However, the subsequent rotation of the folds remained an unresolved question, with geologists using both material line rotation (e.g. Jamison, 1991) or finite strain rotation (Treagus and Treagus, 1992) as an explanation. Physical and numerical experiments helped address these questions. Wilcox *et al.* (1973), Wilson (1970), Graham (1978), Odonne and Vialon (1983) and Richard *et al.* (1991) all produced en échelon folds above a basement detachment fault. As pointed out by Jamison (1991), the plastic material used by Wilcox *et al.* (1973) does not allow any extension and is thus of limited applicability to natural settings. The experiments of Wilson (1970), Graham (1978) and Odonne and Vialon (1983) indicated that folding often starts at approximately 45° to the underlying basement fault, but folds are commonly rotated to a lower angle during deformation. These experimental results were obtained using both wet tissue paper (Wilson, 1970; Graham, 1978) and paraffin wax (Odonne and Vialon, 1983). The experiments of Richard *et al.* (1991) used interlayed Newtonian silicon and sand in order to simulate a combination of brittle and ductile deformation. In this study, folding also initiated at ≈45° to the underlying basement fault and folds rotated during progressive deformation. Folding in these experiments was accompanied by development of both synthetic and antithetic faulting. Because of the nature of all of these physical experiments (under-

*Current address: Department of Geology and Geophysics, Rice University, Houston, TX 77005, U.S.A.

lying strike-slip fault), they could not fully explain the initiation and subsequent rotation of folds for the more general case of transpressional deformation.

Fletcher (1991) and James and Watkinson (1994) created three-dimensional, analytical models for buckle-folded layers, the latter paying particular attention to transpressional deformations. The model of James and Watkinson (1994) suggests that the folds do initiate perpendicular to the shortest infinitesimal strain axis. Unfortunately, their analysis was not applicable to higher strain values, and the subsequent rotation could not be evaluated.

The present physical experiments were designed particularly to address the question of fold initiation and subsequent rotation during transpressional deformation. The experimental apparatus, designed after that of Withjack and Jamison (1986), allowed us to control very closely the kinematics of deformation. Rather than have deformation occur above a basement fault, it occurs on a rubber sheet which acts to homogenize the deformation. The results were compared to theoretically-derived kinematic results, following the method of Fossen and Tikoff (1993). Our results also suggest that folds initially form perpendicular to the infinitesimal contraction direction within the folded layer. We were also able to resolve that the folds rotate with the long axis of the horizontal finite strain ellipse, for the relatively low strains investigated. These results are applied to folds adjacent to the San Andreas fault in central California.

EXPERIMENTAL APPARATUS

An experimental apparatus (Fig. 1) was designed to simulate transpressional folding. This apparatus is based on, but not identical to, the machine used by Withjack and Jamison (1986) to study transtensional deformation. There are two lower metal plates, one of which remains fixed during the deformation. The other plate is connected, by fixed rods below the plates, to a motor. These two plates only move directly towards or away from each other. Sheet metal plates fit on top of these lower metal plates and are fixed by wing-nuts. The acute angle between the sheet metal plates is the angle (α), which is also the angle between the bottom edge of the deforming zone and the movement direction of the sheet metal plates. In our experiments, we used six sheet metal plates cut to represent a given angle of convergence: $\alpha = 0^\circ$, 15°, 25°, 45°, 60° and 90° ($\alpha = 45^\circ$ in Fig. 1).

Homogeneous deformation was provided by a rubber sheet connected to both of the sheet metal plates. A cartoon of deformation is shown in Fig. 2, with respect to stretching of a rubber sheet. The unstretched dimensions of the rubber sheet were 20.5 cm by 5.5 cm, for all angles of convergence, which corresponds to the configuration shown in Fig. 2(a) for $t = 2$. The experiments began with the rubber sheet stretched to its maximum length, which varied between 12 cm (for $\alpha = 90^\circ$) and 5.5 cm (for $\alpha = 0^\circ$) ($t = 0$ in Fig. 2a). Then, the sheet metal pieces begin to move toward each other ($t = 1$ and 2). This arrangement had the advantage that the rubber sheet

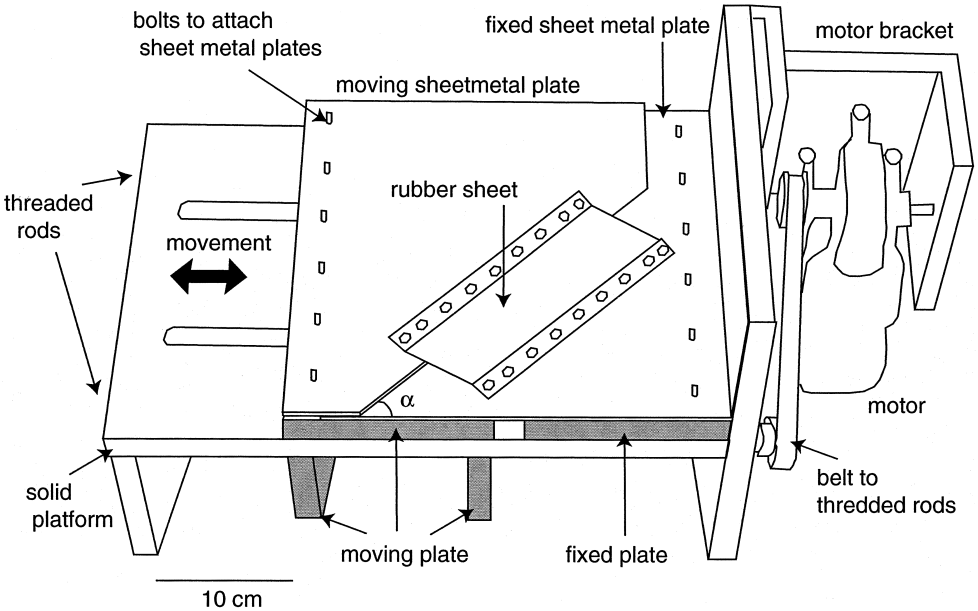

Fig. 1. Line drawing of experimental apparatus. Designed after Withjack and Jamison (1986). Rigid metal plates (shaded) control motion of the overlying sheet metal plates and rubber sheet.

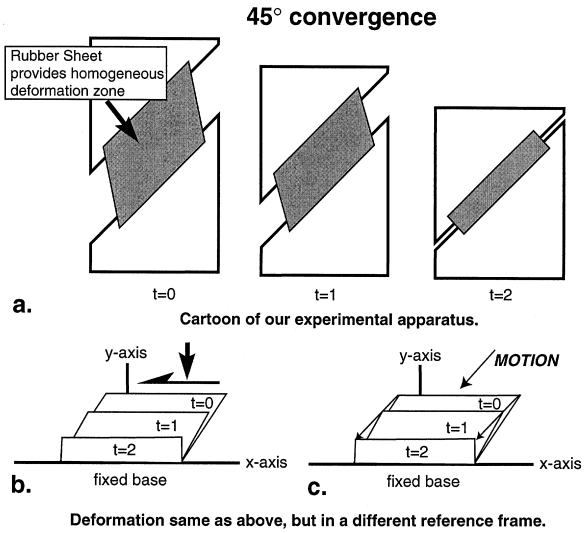

Fig. 2. Cartoon of deformation at three time intervals. (a) Experiment viewed from on top. (b) Experiment viewed parallel to the fixed plate. (c) Horizontal flow lines are always straight and parallel, as required by transpressional kinematics.

was never slack during the final stages of the deformation ($t = 2$).

It is not immediately obvious that the deformation resulting from the experimental apparatus is exactly transpression. The easiest way to envision this deformation as transpressional is to view the deformation parallel to the bottom edge of the rubber sheet (Fig. 2b), not to the moving plate (Fig. 2a). In this case, it is easy to see that one side of the rubber sheet is moving directly toward the other side. In this reference frame, it is clear that the horizontal flow lines of deformation are parallel and straight (Fig. 2c), which is diagnostic of transpression (e.g. Fossen *et al.*, 1994; Tikoff and Teyssier, 1994). Therefore, the corners of the moving plate form a straight line for the three times $t = 0$, 1, and 2 (Fig. 2c). The shear component—dextral for this case—is obvious from observing the sides of the rubber sheet. Displacement rates of the plate were in the range of 0.05–0.1 cm/s for the experiments.

The experiments were conducted with a three-layer model (from bottom to top): rubber sheet, silicone, and a silicone/plasticine mixture. The lower silicone layer (RD-20; Rhone Poulenc) behaves in a Newtonian fashion and 'sticks' to both the overlying plasticine/silicone mixture (even in the anticline hinges) and the underlying rubber sheet. Its role in the experiments was primarily to decouple the rubber sheet and the folding plasticine/silicone layer. The plasticine/silicone layer acts as the stiff layer and folds during deformation. The exact mixture of plasticine and silicone was controlled simply by what folded well, although all experiments were conducted with a single mixture. Based on fold shapes from the pure convergence experiments ($\alpha = 90°$), Lan (personal communication, 1995) estimated the power-law exponent for the silicone/plasticine mixture as $n = 6.5$–8 using the method of Hudleston and Lan (1994). Note that this estimation assumes that the silicone/plasticine mixture is a viscous material with a power-law rheology, whereas it may be better described as a visco-elastic rheology. The silicone/plasticine layer was initially 0.3–0.5 cm thick.

Finally, a grid and a round marker were placed on the plasticine/silicone layer (Figs 3 & 4). This was done by tracing a grid and a circle on a regular sheet of paper, and placing that sheet of paper face down on the experiment, thus transferring the graphite to the top of the plasticine/silicone layer. Since the marks were superficial, they acted as passive markers with no mechanical effect.

EXPERIMENTAL RESULTS

The experiments were recorded on videotape, through the use of low-angle lighting, and subsequently analyzed on computer. The results of two angles of convergence are shown: Fig. 3 ($\alpha = 0°$) and Fig. 4 ($\alpha = 45°$). Also, a cross-section is shown for the $\alpha = 45°$ convergence experiments (Fig. 5). Approximately four experiments were run for each angle of convergence and the most uniform experiment was chosen to analyze the results. Folding was first visible when finite strain ellipse ratio in the horizontal plane, calculated theoretically based on offset, was $R \sim 1.13$–1.35. The thickening of the basal silicone layer occurs simultaneously with folding of the stiff plasticine/silicone layer.

The folds analyzed in the 45° angle of convergence are shown in Fig. 6. The dashed lines are the traces of the fold hinges that were used in the calculations, which mostly lie in the middle of the rubber sheet. Three areas of folding were avoided in our analyses: (1) Folds near the sides of the rubber sheet. This area was avoided because of the tendency for the rubber sheet to slightly 'neck' or thin ('Poisson effect') when extended; (2) Folds which propagated off the nuts which held the rubber sheet in place on the bottom and top of the deforming zone; and (3) Folds in the 'corner' zones which were varied in orientation and deformation style (e.g. slightly recumbent). As is seen in the results (Figs 3, 4 & 6), the orientation did not vary much even in these areas.

After these experimental results were analyzed, the theoretical curves for finite strain were produced using a kinematic model of transpressional deformation (e.g. Fossen and Tikoff, 1993). The kinematics of transpression are justified by the imposed boundary conditions and the lack of sideways extrusion observed during the experiments. Further, we emphasize that these calculations are for homogeneous isotropic deformation, which do not specifically address any dynamics of the folding process. Two different kinematic models for fold orientation were calculated: (1) parallel to the orientation of the horizontal finite strain axes; and (2)

parallel to the rotation of a material line. Both the finite strain axes and material line rotation initiate at the same angle, parallel to the infinitesimal strain axes, although their subsequent orientations are different. In general, the rotation of the material line is faster than the finite strain axes. This result is particularly clear for a low angle of convergence ($\alpha \leq 25^\circ$), which provides the largest differences in rotation between finite strain axes and material line rotation.

The results of all analyzed folds and the average fold trend are plotted in Fig. 7, against the theoretically derived values, for each angle of convergence. All angles of convergence in all experiments suggest that the fold hinge is parallel to the long axis of the horizontal finite strain ellipse (Fig. 7). In these cases, the average trend lies extremely near the expected value for the horizontal finite strain axes. In fact, only rarely do any of the fold orientations fall below the predicted material line rotation. The results for the higher angles of convergence ($\alpha = 45^\circ$ and 60°) are slightly more ambiguous, simply because there is only a few degrees difference between the two theoretical curves. However, these results also generally support the notion that the rotation parallels the finite strain axes (e.g. Treagus and Treagus, 1992). The results for $\alpha = 90^\circ$ were not plotted since the fold hinges remained parallel to the edge of the rubber sheet throughout deformation.

Rotation of material through fold hinges

As noted above, material line rotation is typically faster than finite strain axes rotation. This effect is evidenced, for instance, by the ability of material lines to rotate through the long axis of the finite strain ellipse for simple shear deformations (e.g. Ramsay, 1967). However, given that the fold hinges in transpression rotate with the horizontal finite strain ellipse, the more quickly moving material lines must rotate over the hinge of the fold. This effect was never observed directly in our experiments, primarily because the difference between these two angles is difficult to assess at the low experimental strain values, but is the natural outcome of the analysis.

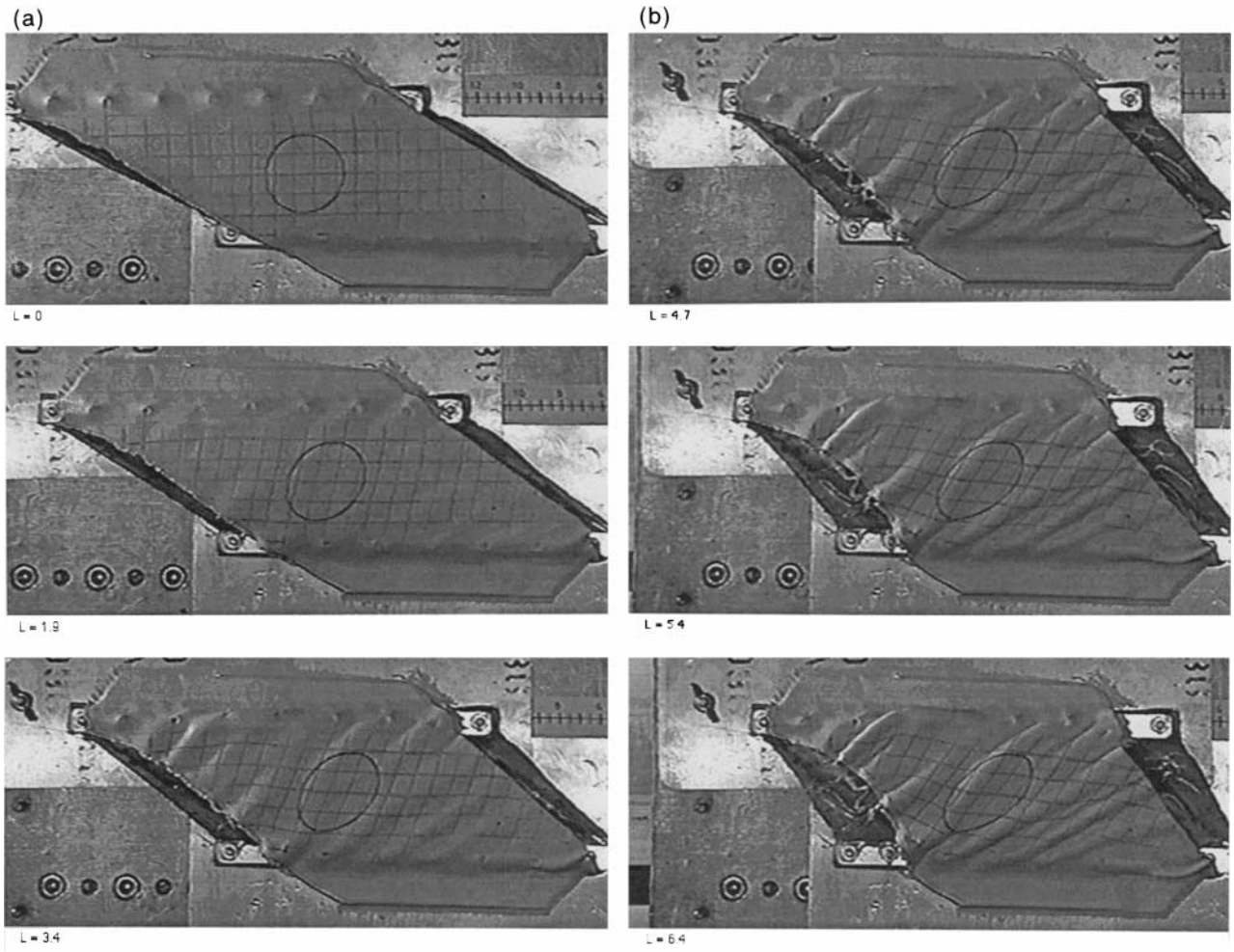

Fig. 3. Experimental deformation for a simple shear experiment ($\alpha = 0^\circ$). The deformation is dextral. A grid and a circle were placed on the uppermost plasticine/silicone layer. L is the amount of displacement in the experiment.

Scatter of data

Odonne and Vialon (1983) note that the initial dispersion of folds formed above their basement fault does not decrease with increasing deformation. Alternatively stated, the scatter in the fold orientation data did not decrease during offset in their experiments. We notice the same lack of clustering in our experiment (Fig. 7). No angle of convergence produces a significant decrease in the angular spread of the data with increasing deformation. Some deformations, notably the 45° convergence, show an increase in the scatter of fold hinge orientation with increasing deformation. Presently, we do not fully understand this effect.

Marker on plasticine/silicone layer

The passive, circular markers (Figs 3 & 4) on the top of the plasticine/silicone layer allowed us to plot the theoretical ratio of the finite strain ellipse vs the graphite ellipse *magnitude* (Fig. 8). These markers were designed to encompass several folds, in order to get an 'average' strain and discount the bending strains associated with any individual fold. In terms of magnitude of the axial ratio, the graphite ellipse fell below

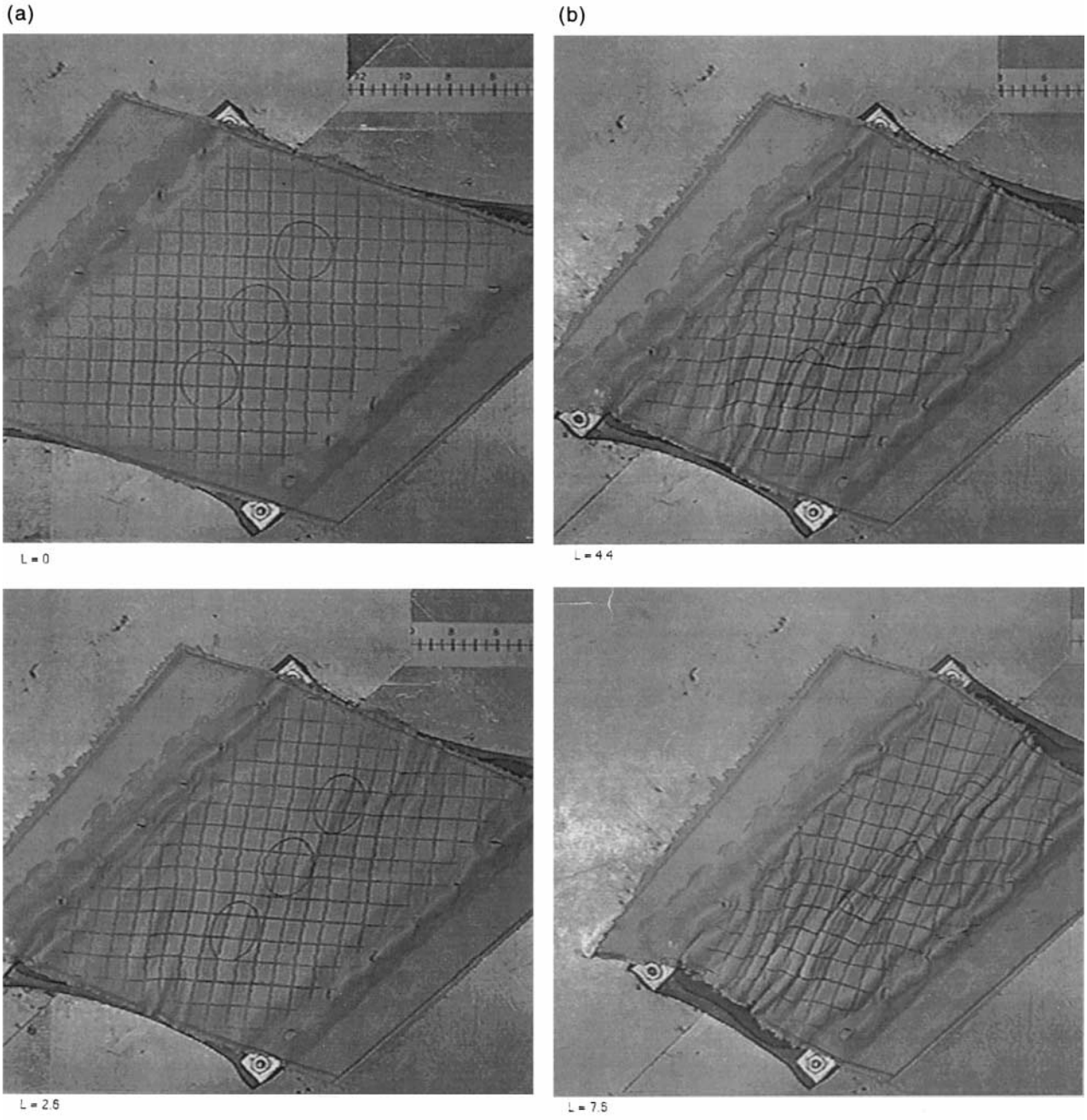

Fig. 4. Experimental deformation for a convergence angle (α) of 45°. The deformation is dextral shear combined with contraction. L is the amount of displacement in the experiment.

the theoretical value for the $\alpha = 0^\circ$ experiments, but not for the higher convergence angle experiments (such as $\alpha = 45^\circ$).

The wrench experiment ($\alpha = 0^\circ$) was repeated with a less viscous plasticine layer that deformed homogeneously (i.e. it did not fold) and the agreement with the theoretical value is quite good. On examination of the simple shear experiment (Fig. 3), a partial explanation of this effect is apparent. During the course of the experiment, there is stretching of the graphite circle as evidenced by the elongation of the graphite ellipse from its original length. However, the extension is not fast enough to match the movement, and the 'sides' of the experiment tend to pull inward. Thus, the final length of the entire deforming zone is not as long as the original length. Because of this effect, some care is needed in interpreting the results of the simple shear experiments.

EXPERIMENTAL ANALYSIS

Determination of infinitesimal strain (stress) and finite strain from folds

Fossen and Tikoff (1993) and Tikoff and Teyssier (1994) define two types of transpression, based on the orientation of the infinitesimal strain axes: wrench-dominated and pure-shear dominated. In wrench-dominated transpression, $\dot{s}_1$ and $\dot{s}_3$ lie in the horizontal plane and oblique to the shear plane, while $\dot{s}_2$ is vertical. In pure-shear dominated transpression, $\dot{s}_2$ and $\dot{s}_3$ lie in the horizontal plane and are oblique to the shear (x–z) plane, and $\dot{s}_1$ is vertical. Wrench-dominated transpression corresponds to angles of convergence $0^\circ < \alpha < 20^\circ$ and pure-shear dominated transpression corresponds to $20^\circ \leq \alpha < 90^\circ$. In terms of the development of experimental folds, no difference was seen

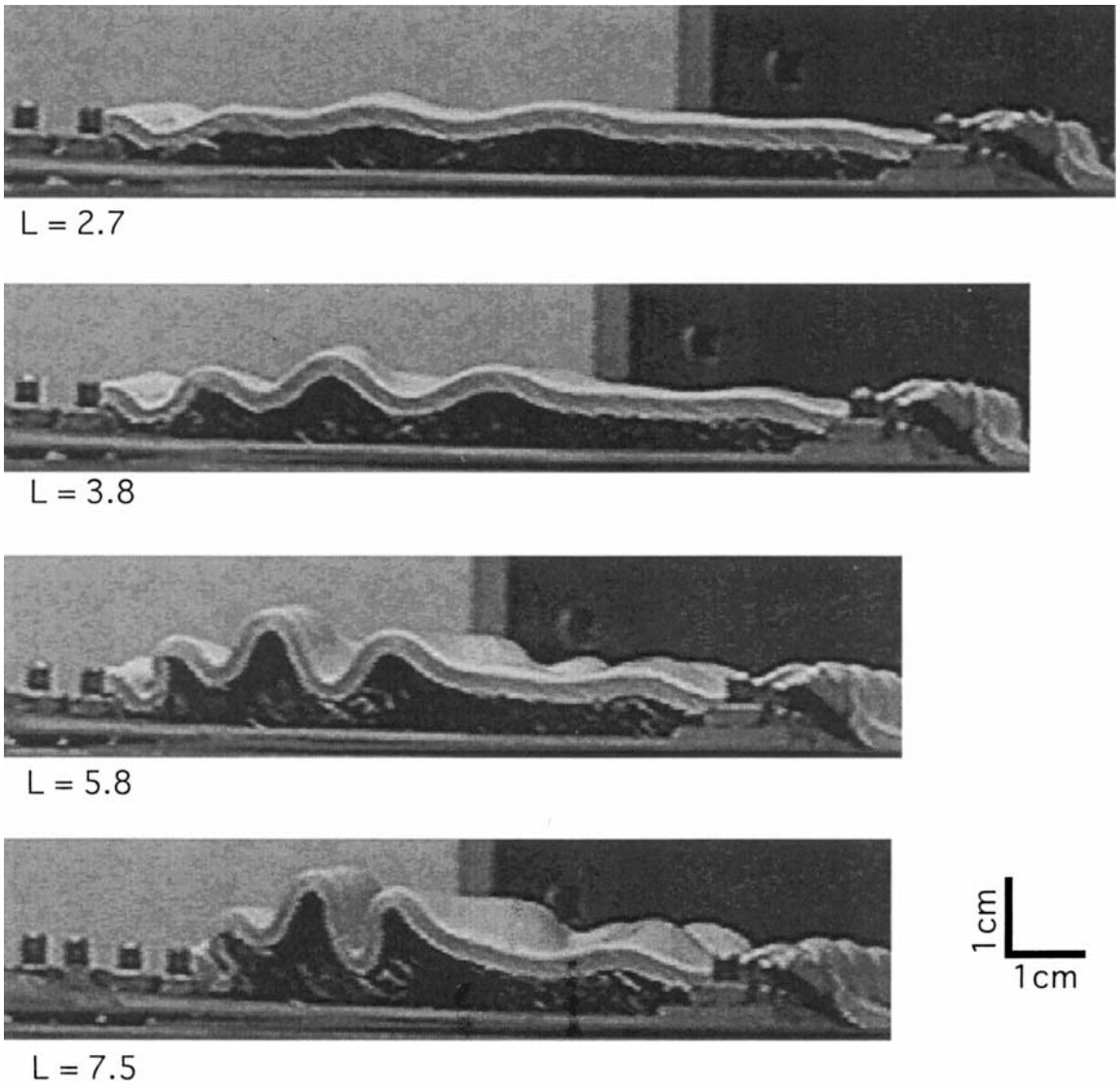

Fig. 5. Cross-sectional view of experimental deformation for a convergence angle (α) of 45° (same experiment as Fig. 4). The diagrams are side views from a single progressive deformation, and there was no sectioning of the material. Thickening of basal silicone occurs simultaneously with folding.

between the wrench-dominated experiments ($\alpha = 0°$, 15°) and the pure-shear dominated experiments. In both cases, the hinges of the fold axes tracked the maximum horizontal finite strain axis.

There are also two possible orientations for the finite strain axes for transpressional deformations (e.g. Fossen and Tikoff, 1993). S_2 and S_3 lie in the horizontal plane, and S_1 is vertical, for all cases of pure-shear dominated transpression and some cases of wrench-dominated transpression. S_1 and S_3 lie in the horizontal plane, and S_2 is vertical for some cases of wrench-dominated transpression. The former case (S_2 and S_3 lie in the horizontal plane) is favored for wrench-dominated transpression with angles of convergence close

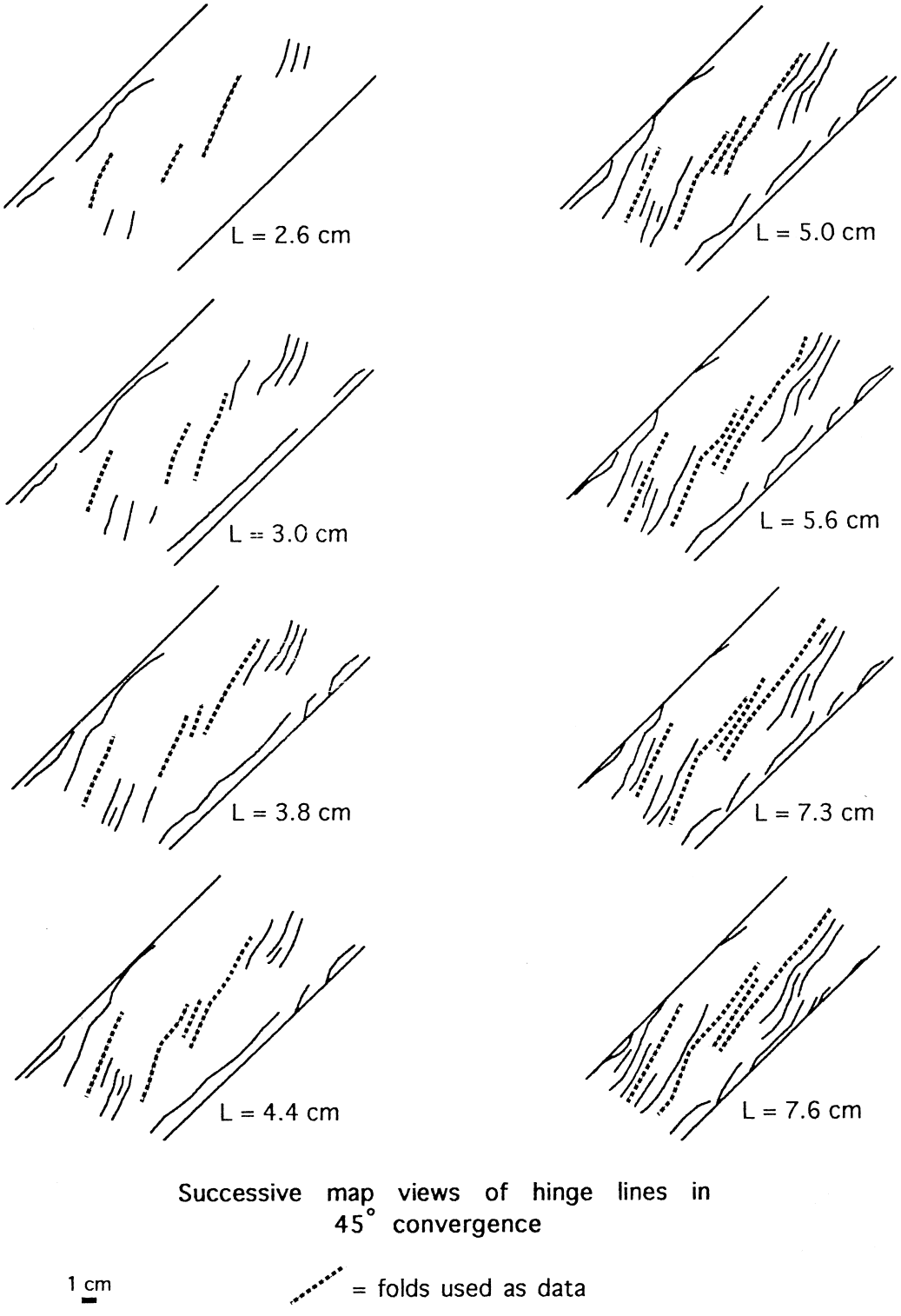

Fig. 6. Folds used in the analysis, for $\alpha = 45°$ (same experiment as Fig. 4). Folds (dashed lines) near the middle were used for analysis (see text). Although not used in the analysis, folding in other areas is sub-parallel to folding in center.

to 20° or high strain zones (Tikoff and Greene, 1997). No significant difference is found in our experiments between these two cases.

If a rheology is assumed, one can also correlate infinitesimal strain with stress, which is routinely done in neotectonic studies. However, as observed within our models of folds in a transpressional setting, neither the infinitesminal or finite strain can be determined solely on the final shape of the fold (Fig. 9). Consequently, no inference about the 'regional' stress direction is possible from fold geometry alone. Rather, there are three possibilities of stress and strain relations within folds in transpressional settings (Fig. 9).

Lack of three-dimensional rotation

As indicated by kinematic modeling, the long axis of the finite strain ellipsoid is often vertical for transpressional deformations (e.g. Sanderson and Marchini, 1984). Further, Fossen and Tikoff (1993) illustrated that any material line that does not lie exactly in the horizontal plane should rotate into a vertical orientation for transpressional deformations. Therefore, we would expect that some fold hinges would begin to rotate toward a vertical orientation.

In the physical experiments, for a variety of convergence angles, some fold axes on the edges of the rubber sheet initiated with angles that deviated ~5–10° from horizontal. Yet, these fold axes did not progressively steepen during deformation. This result corroborates the notion that the fold hinges do not rotate as material lines. If the material was passively responding to bulk transpression kinematics, we would expect some upward movement and subsequent steepening of the gently-plunging fold axes. The most likely explanation is that the stiff layer develops a structural anisotropy as a response to folding (e.g. Cobbold and Watkinson, 1981), which prevents the hinges from behaving as passive material lines.

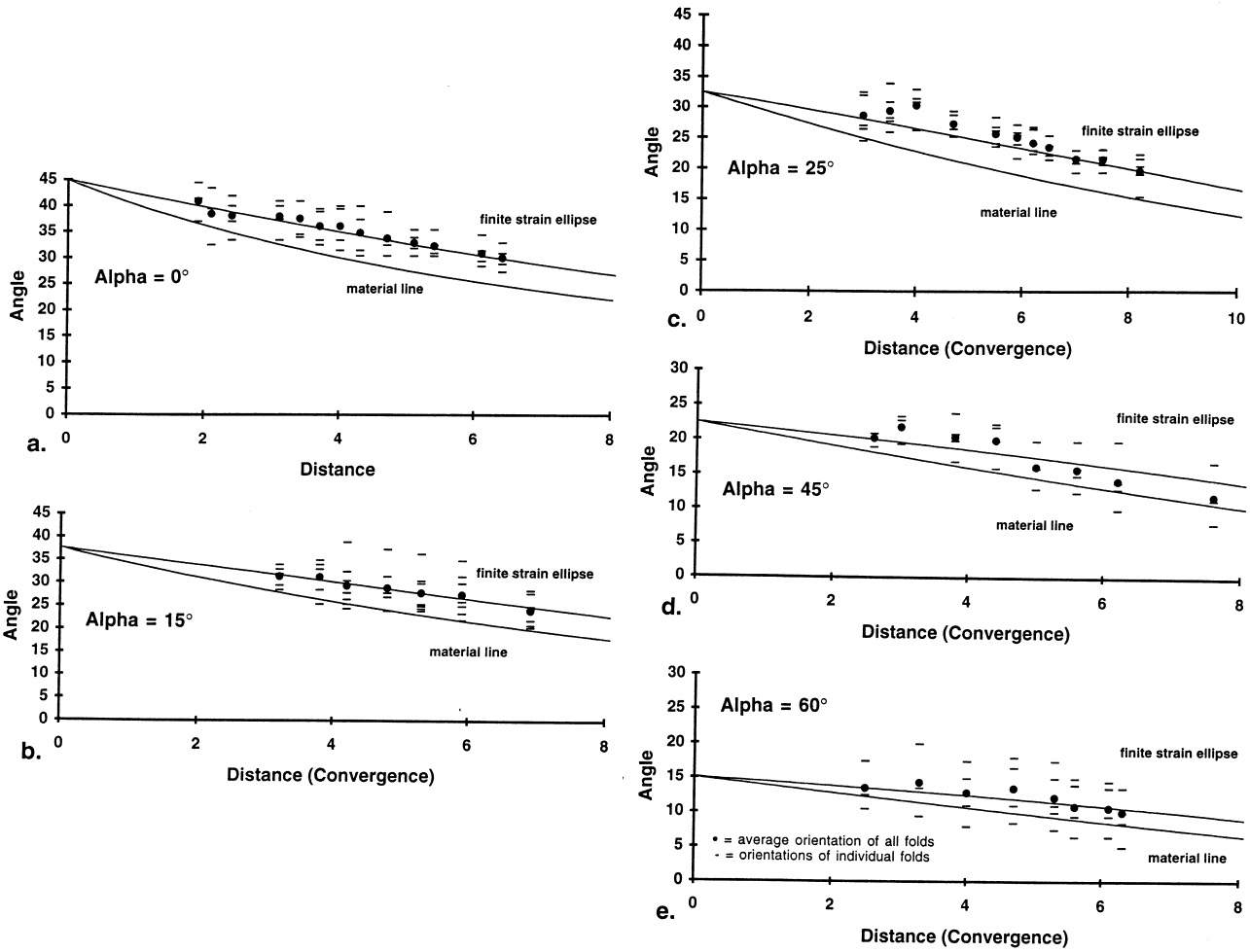

Fig. 7. Orientation of folds plotted against the amount of convergence, for all angles of convergence. Dashes represent individual folds and filled circles represent average values. Also plotted are the theoretical values of the horizontal finite strain ellipse and the rotation of a material line (assumed to start parallel to the infinitesimal extension direction). All experiments suggested that folds rotate parallel with the horizontal finite strain ellipse.

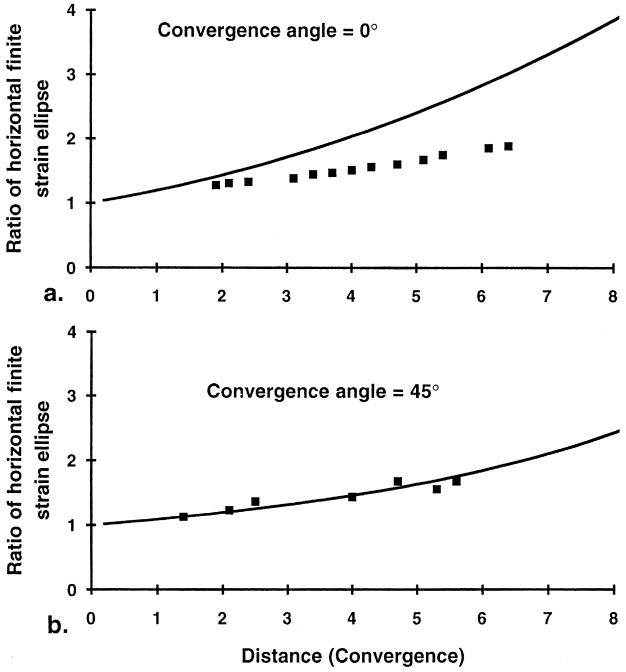

Fig. 8. Magnitude (not orientation) of deformation of a passive marker against theoretical prediction, for $\alpha = 0°$ (Fig. 3) and 45° (Fig. 4). The divergence from predicted values for wrenching ($\alpha = 0°$) is a result of insufficient horizontal stretching (see text).

Overestimation of contractional deformation and hinge-parallel extension

As indicated by Jamison (1991), all folds in transpression should accommodate a certain amount of extension parallel to the fold hinges. This behavior is inferred in the analytical model of James and Watkinson (1994) and observed, in the form of normal faults sub-perpendicular to the fold hinges, in the physical experiments of Richard *et al.* (1991). Hinge-parallel extension increases with decreasing convergence angle, and is particularly acute for simple shear ($\alpha = 0°$). In this case, all of the contraction indicated by the folding is matched by extension parallel to the fold hinges. Only by the material reacting in this way can the wrench deformation remain plane strain (i.e. two-dimensional).

In our experiments, the folding material (plasticine/silicone) was unable to deform by brittle deformation. Hence, no extensional cracks sub-perpendicular to the fold hinges were observed, which would correspond to hinge-perpendicular normal faulting or boudinage in natural examples of transpressional folding (Jamison, 1991; Bürgmann, 1991). Rather, because the silicone/plasticine layer is capable of stretching, it deformed by ductile thinning (although not quickly enough in the simple shear experiments; see above). Extension parallel to the fold axes is seen by elongation of the circular marks in Figs 3 and 4.

Figure 5 shows a cross section of the folding experiment for $\alpha = 45°$. A percentage of the observed shortening is real, but some is counter-balanced by ductile extension. Thus, the hinge-parallel extension remains an important point for balancing cross-sections in transpressional areas. Although cross-sections in transpressional settings may indicate large amounts of contraction, they will overestimate the true amount of contraction.

APPLICATION TO CENTRAL CALIFORNIA

The well-documented transpressional tectonics in central California provide an opportunity to apply the experimental results. A switch from a transcurrent/transtensional to transpressional deformation occurred in central California at 3.4–3.9 Ma, as a result of minor changes in relative plate motions (Harbert, 1991). In this location, the rate of plate convergence between the North America and Pacific plates is 48.0 mm/y at approximately 5°, which is resolvable into transcurrent (47.8 mm/y) and normal (4.2 mm/y) components (DeMets *et al.*, 1990).

However, distributed dextral deformation occurs in the borderland regions of the San Andreas fault system (Jamison, 1991). In these areas, en échelon folds and faults are commonly observed (e.g. Diblee, 1976; Harding, 1976) flanking the major strike-slip faults. Deformation in the wrench borderlands of the San Andreas fault system is well studied by field mapping, drill cores, and seismic sections (e.g. Namson and Davis, 1988; Namson and Davis, 1990; Bloch *et al.*, 1993). Using this data, Bloch *et al.* (1993) estimated

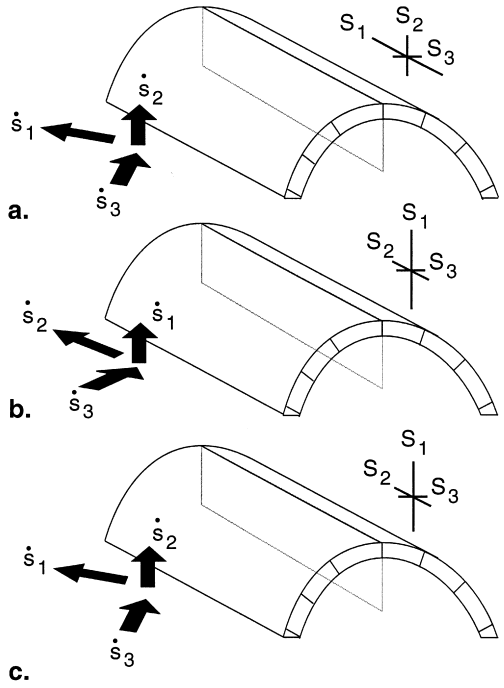

Fig. 9. Cartoon of three orientations for infinitesimal strain (stress) and finite strain in our experiments. There was no difference in folding behavior for different orientations of strain axes.

contraction of 33.1 km on a cross-section perpendicular to the fold hinges, based on a décollement at 11–14 km depth. Because contractional deformation initiated at ≈3.4 Ma, one can calculate margin-normal convergence rate of 9.2 mm/y. Thus, the contraction rate is over double the plate motion-derived contraction rate of 4.2 mm/y.

The contraction across the San Andreas system is overestimated by not considering the hinge parallel stretching of the oblique folds (Jamison, 1991; Krantz, 1995). The simple shear experiments of the folding exhibit this same effect. Viewed across the strike of the folds, one would estimate large amounts of contraction. However, this contraction is exactly counterbalanced by hinge parallel extension for pure wrenching to arrive at the required 'bulk' plane strain deformation. A particularly good example of hinge-parallel stretching adjacent to the San Andreas fault was provided by Bürgmann (1991), who documented the boudinage of an ash layer along the hinge of a fold in Southern California (Durmid Hills).

If the angle of convergence and the amount of contraction are known, the effect of hinge parallel stretching can be calculated. Figure 10 indicates the ratio of horizontal extension to contraction rates, for all angles of convergence in a transpressional deformation. Since this effect is caused by the wrench component of deformation, it decreases away from $\alpha = 0^\circ$ and does not exist at $\alpha = 90^\circ$. The transition from wrench-dominated to pure-shear dominated transpression is designated by $\alpha = 20^\circ$, which correlates to a switch in orientation of $\dot{s}_1$ and $\dot{s}_2$. For this convergence angle, the rate of extension in the horizontal and vertical directions are equal, and exactly one half of the horizontal contraction is compensated by horizontal extension (horizontal extension/horizontal contraction = 0.5). For intermediate values, for example $\alpha = 30^\circ$, the true amount of contraction is simply the amount of contraction not compensated by vertical extension (horizontal extension/horizontal contraction = 0.3). The wrench component of deformation may be calculated using the angle of convergence and the amount of normal contraction.

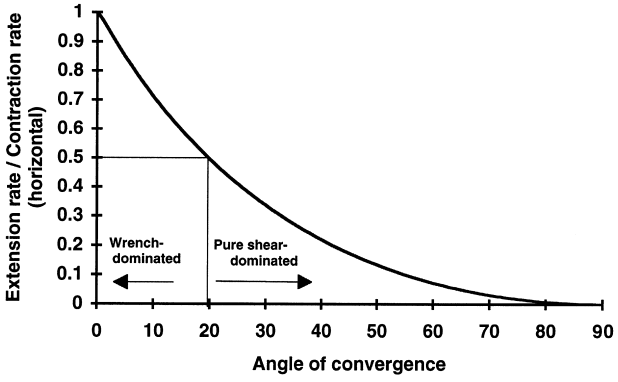

Fig. 10. Graph of infinitesimal horizontal stretching ($\dot{s}_1$) or ($\dot{s}_2$) to infinitesimal horizontal contraction ($\dot{s}_3$), as a function of angle of convergence for transpressional deformations. Because horizontal contraction is partially accommodated by a component of horizontal extension, balanced cross-sections in transpressional zones will tend to overestimate true contraction. This effect is most acute for low angles of convergence (wrench-dominated transpression), in which over 50% of contraction is accommodated by horizontal extension.

Teyssier and Tikoff (in press), using the strike-slip partitioned model of Tikoff and Teyssier (1994), estimate that the angle of plate motion in the wrench borderlands of the San Andreas fault is $\alpha = 20^\circ$. If this analysis is correct and there is 33.1 km of 'apparent' contraction across the San Andreas fault, one can calculate an actual contraction across the fault of 16.6 km. This provides a normal contraction rate of 4.6 mm/y, which is comparable to the convergence rate predicted by plate motion (4.2 mm/y). The analysis also suggests that a large amount of transcurrent motion occurs as wrench deformation in California (12.7 mm/y), which may account for the missing tangential motion or San Andreas 'discrepancy' (calculated at 12.8 mm/y from plate motion) (see Teyssier and Tikoff, in press).

This analysis is intriguing because $\alpha = 20^\circ$ corresponds to the transition between wrench-dominated and pure-shear dominated transpression. If the above analysis is correct, the orientation of the finite strain axes are determined (S_2 and S_3 in the horizontal plane, S_1 vertical), but the orientation of the infinitesimal strain axes (stress) are not (Fig. 9b or c). Given the uncertainties in the plate motion models, our analysis should be considered tentative. However, the important result remains the same: a component of transcurrent plate motion is accommodated in the folded wrench borderland adjacent to the San Andreas fault. This wrench component also causes an overestimation of contraction seen in cross-sections, by not considering the hinge-parallel extension.

DISCUSSION

The role of the basal layer

The rheology of the basal silicone layer is very important to the process of folding. As seen in Fig. 5, the basal silicone layer thickened during the experimental deformation, as it was pushed together by the rubber sheet. Therefore, the overlying plasticine/silicone layer not only folded, but the average height of the layer increased during deformation. This effect was most pronounced in pure convergence ($\alpha = 90^\circ$) and non-existent for pure wrenching ($\alpha = 0^\circ$). Another obvious effect is that the basal silicone sticks everywhere to the overlying plasticine/silicone layer. This requires the existence of relatively high shear strains, as silicone is sheared into the growing anticlines and away from the synclines. In the same way that the basal silicone layer sticks to the overlying layer, it also sticks to the underlying rubber sheet.

Experiments were also conducted to determine the role of the Newtonian silicone in the experiment (e.g. coupling vs decoupling). In these experiments, the plasticine/silicone only overlay the basal silicone (e.g. the plasticine/silicone did not overlap onto the rigid plates). Folding did not occur in these cases. Rather, the plasticine/silicone layer remained flat and rigid during deformation. This behavior requires that the basal silicone 'decouples' the folding layer and the rubber sheet during the experiment. However, this result is only applicable to the plasticine/silicone layer used in the folding experiments. The same experiment was also conducted with sand overlying on the silicone layer, in which case the sand did deform. It should be noted that the sand did mix with the silicone at their interface, which may have effected the coupling between the layers. Regardless, this observation requires that the Newtonian silicone at least partial couples the rubber sheet and the overlying sand. Thus, the general role of the silicone in coupling or decoupling depends on the mechanical behavior of the overlying material and the interface between the layers.

Evaluation of folds in the field

Figure 9 illustrates the possible orientations of our experimental folds compared to the infinitesimal and finite strain axes. In pure shear-dominated transpression, the long axis of the finite strain ellipsoid (S_1) and the infinitesimal extension direction ($\dot{s}_1$) are vertical. The short axis of the finite strain ellipsoid (S_3) and the infinitesimal contraction direction ($\dot{s}_3$) both lie in the horizontal plane, but are not parallel because of the wrench component of deformation. For wrench dominated transpression, particularly low strain and low angles of convergence, both S_1 and $\dot{s}_1$ lie in the horizontal plane, as well as S_3 and $\dot{s}_3$. Again, these quantities are not parallel except during the first (and undetectable) increment of deformation. For cases of wrench dominated transpression, both $\dot{s}_1$ and $\dot{s}_3$ lie in the horizontal plane, although S_1 is vertically oriented (e.g. Fossen and Tikoff, 1993).

In all cases, the resultant fold may have the same appearance, particularly in cross-section. However, there are some differences. As demonstrated by Bürgmann (1991), there is a significant component of hinge-parallel extension if the deformation approaches pure wrenching. This hinge-parallel extension decreases as the angle of convergence increases (Fig. 10). Unfortunately, hinge-parallel extension is generally difficult to quantify.

Finite strain measurements may be used to distinguish between these cases. In fact, the observation of long axes of the finite strain ellipsoid parallel to fold hinges is easily explained by wrench-dominated transpression. However, the difficulty with this approach is that the process of folding also causes local strain (e.g. outer-arc extension). Therefore, regional fabrics are commonly superimposed on folding fabrics, obscuring the tectonic relationships (e.g. Hudleston *et al*., 1988).

We believe the best approach is that suggested by Jamison (1991) which involves investigation of large-scale patterns of folding. Thus, if steady-state deformation is assumed (i.e. constant angle of convergence), one can determine the kinematics of folding by knowledge of any three of these parameters: (1) the orientation of the boundary of deformation (typically a major fault of plate contact); (2) fold axes orientation; (3) amount of contraction recorded by the folds; (4) true contraction across the deforming zone; (5) amount of hinge-parallel extension; (6) amount of vertical extension; (7) direction of convergence; and (8) direction of infinitesimal contraction. As indicated by Jamison (1991), the amount of fold-perpendicular contraction may be estimated by using limb dips of folded layers.

Future work

At present, we do not understand two major aspects of our folding experiments. First, the scatter of the fold hinge orientation remains large, or possibly increased, during the course of the deformation. Because material lines should cluster parallel to the extensional finite strain axis during deformation, we would expect folds to respond in the same way. Secondly, we expected more three-dimensional rotation of fold hinges to occur. Again, passive material lines that initiate with a slight orientation to the horizontal plane should rotate into a vertical orientation during transpressional deformation, however they do not. Both of these observations support the hypothesis that folds do not rotate as material lines, but rather the process of folding creates a bending anisotropy (Cobbold and Watkinson, 1981). This process could have implications for *in situ* stress measurements in obliquely convergent settings, as the stiff folded layers may induce an anisotropy and act as stress guides.

Additionally, we emphasize the relatively low strains involved in these experiments. At higher strains, it is possible the rotation of fold hinges will approach that of material lines (e.g. Jamison, 1991). In these cases, fold hinges will invariably rotate toward the largest axis of the finite strain ellipsoid, parallel to the stretching lineation (e.g. Cobbold, 1976). However, as indicated above, this scenario does not describe all cases of folding with stretched hinges (e.g. Watkinson, 1975).

CONCLUSION

Folds were created within a shear box, in a single stiff layer of mixed plasticine and silicone. Homogeneous transpression was attained by the use of

a rubber sheet and a layer of basal silicone. The fold hinges rotated parallel to the long axis of the horizontal finite strain ellipse for a variety of convergence angles ($\alpha = 0^\circ$, 15°, 25°, 45°, 60° and 90°), although the effect was best observed for low angles of convergence. One caveat is that, for the simple shear experiment, the folding layer did not extend as quickly as contraction occurred.

Analysis of the results suggests that there are three basic relationships between the orientations of infinitesimal strain (stress) and finite strain for transpressional deformation zones. Further, balancing cross-sections in areas of transpressional folding will tend to overestimate the amount of contraction across the zone by not considering the hinge parallel extension. This result is shown for an area of central California.

Acknowledgements—Peter Hudleston and Labao Lan are gratefully acknowledged for helpful conversations about folding and Christian Teyssier is acknowledged for logistical and scientific support. P. Richard and J. Watkinson are thanked for helpful reviews. Ron Bohm and Lee Nelson, in basement of Pillsbury Hall, built the apparatus and tolerated an endless amount of tinkering with it: Many thanks. Supported by NSF EAR-9607018.

REFERENCES

Bloch, R. B., Huene, R. V., Hart, P. E. and Wentworth, C. M. (1993) Style and magnitude of tectonic shortening normal to the San Andreas fault across the Pyramid Hills and Kettleman Hill South Dome, California. *Bulletin of the Geological Society of America* **105,** 464–478.

Bürgmann, R. (1991) Transpression along the Southern San Andreas fault, Durmid Hill, California. *Tectonics* **10,** 1152–1163.

Cobbold, P. R. (1976) Fold shapes as functions of progressive strains. *Philosophical Transactions of the Royal Society of London* **A328,** 129–138.

Cobbold, P. R. and Watkinson, A. J. (1981) Bending anisotropy: a mechanical constraint on the orientation of fold axes in an anisotropic medium. *Tectonophysics* **190,** 209–232.

DeMets, C., Gordon, R. G., Argus, D. F. and Stein, S. (1990) Current plate motions. *Geophysics Journal International* **101,** 425–478.

Diblee, T. W. (1976) The Rinconda and related faults in the southern Coast Ranges, California, and their tectonic significance. *U.S. Geological Survey Professional Paper* **981**.

Fletcher, R. C. (1991) Three-dimensional folding of an embedded viscous layer in pure shear. *Journal of Structural Geology* **13,** 87–96.

Flinn, D. (1962) On folding during three-dimensional progressive deformation. *Quarterly Journal of the Geological Society of London* **118,** 385–428.

Fossen, H. and Tikoff, B. (1993) The deformation matrix for simultaneous pure shear, simple shear, and volume change, and its application to transpression/transtension tectonics. *Journal of Structural Geology* **15,** 413–425.

Fossen, H., Tikoff, B. and Teyssier, C. (1994) Strain modeling of transpressional and transtensional deformation. *Norsk Geologisk Tidsskrift* **74,** 134–145.

Graham, R. H. (1978) Wrench faults, arcuate fold patterns and deformation in the southern French Alps. *Proceedings of the Geological Association* **89,** 124–142.

Harbert, W. (1991) Late Neogene relative motions of the Pacific and North American plates. *Tectonics* **10,** 1–16.

Harding, T. P. (1976) Tectonic significance and hydrocarbon trapping consequence of sequential folding synchronous with San Andreas faulting, San Joaquin Valley, California. *Bulletin of the American Association of Petroleum Geologists* **60,** 356–378.

Harland, W. B. (1971) Tectonic transpression in Caledonian Spitsbergen. *Geological Magazine* **108,** 27–42.

Hudleston, P. J., Schultz-Ela, D. and Southwick, D. L. (1988) Transpression in an Archean greenstone belt, northern Minnesota. *Canadian Journal of Earth Sciences* **25,** 1060–1068.

Hudleston, P. J. and Lan, L. (1994) Rheological controls on the shapes of single-layer folds. *Journal of Structural Geology* **16,** 1007–1021.

Jamison, W. R. (1991) Kinematics of compressional fold development in convergent wrench terranes. *Tectonophysics* **190,** 209–232.

James, A. I. and Watkinson, A. J. (1994) Initiation of folding and boudinage in wrench shear and transpression. *Journal of Structural Geology* **16,** 883–893.

Krantz, R. W. (1995) The transpressional strain model applied to strike-slip, oblique-convergent and oblique-divergent deformation. *Journal of Structural Geology* **17,** 1125–1137.

Namson, J. S. and Davis, T. L. (1988) Seismically active fold and thrust belt in the San Joaquin Valley, central California. *Bulletin of the Geological Society of America* **100,** 257–273.

Namson, J. S. and Davis, T. L. (1990) Late Cenozoic fold and thrust belt of the southern Coast Ranges and Santa Maria basin, California. *Bulletin of the American Association of Petroleum Geologists* **74,** 467–492.

Odonne, F. and Vialon, P. (1983) Analogue models of folds above a wrench fault. *Tectonophysics* **99,** 31–46.

Richard, P., Mocquet, B. and Cobbold, P. (1991) Experiments on simultaneous faulting and folding above a basement wrench fault. *Tectonophysics* **188,** 133–141.

Sanderson, D. and Marchini, R. D. (1984) Transpression. *Journal of Structural Geology* **6,** 449–458.

Teyssier, C. and Tikoff, B. Strike-slip partitioned transpression of the San Andreas fault system: a lithospheric model. Transpression/transtension. *Geological Society of London Special Publication* (in press).

Tikoff, B. and Teyssier, C. (1994) Strain modeling of displacement-field partitioning in transpressional orogens. *Journal of Structural Geology* **16,** 1575–1588.

Tikoff, B. and Greene, D. (1997) Stretching lineations in transpressional shear zones. *Journal of Structural Geology* **19,** 29–40.

Treagus, J. E. and Treagus, S. H. (1992) Transected folds and transpression: how are they related? *Journal of Structural Geology* **14,** 361–367.

Watkinson, A. J. (1975) Multilayer folds initiated in bulk plane strain with the axis of no change perpendicular to the layering. *Tectonophysics* **28,** T7–T11.

Wilcox, R. E., Harding, T. P. and Seely, D. R. (1973) Basic wrench tectonics. *Bulletin of the American Association of Petroleum Geologists* **57,** 74–96.

Wilson, G. (1970) Wrench movements in the Aristarchus region of the Moon. *Proceedings of the Geological Association* **81,** 595–608.

Withjack, M. O. and Jamison, W. R. (1986) Deformation produced by oblique rifting. *Tectonophysics* **126,** 99–124.